Low-temperature photoluminescence of germanium doped with arsenic, phosphorus, or antimony

M. V. Gorbunov and A. S. Kaminskiĭ

Institute of Radio Engineering and Electronics, USSR Academy of Sciences
(Submitted 23 May 1984)
Zh. Eksp. Teor. Fiz. **88**, 852–866 (March 1985)

The low temperature luminescence of germanium doped with arsenic, phosphorus, and antimony and deformed in the [001] and [111] directions is investigated. It is shown that in samples with low impurity content the main contribution to the emission is made by exciton-impurity complexes formed on individual atoms. A simplified model of multiparticle exciton-impurity complexes (MEIC) is considered and can explain the changes produced in the spectral distribution of the MEIC recombination radiation under uniaxial deformation of the germanium crystals. It is found that the exciton can be bound to an excited donor. The deformation of the germanium crystals alters the character of the MEIC carrier interaction responsible for the fine splitting of the radiation lines. When the density of the impurity centers is increased, new bands appear in the luminescence spectrum and become dominant at impurity densities $\sim 10^{15}$ cm^{-3}. These lines are inhomogeneously broadened towards the long-wave side and their maxima are shifted ~ 1 meV down in energy relative to the corresponding bound-exciton lines. The new lines appear at densities such that the interactions of the bound excitons with their surrounding centers come into play. This is attested to by the noticeable broadening of the bound-exciton lines at such densities. It is shown that this radiation can be explained as being due to radiative decays of excitons bound to donor pairs.

1. INTRODUCTION

A systematic investigation of the low-temperature luminescence of germanium doped with group III or V elements was initiated by Gross, Novikov, and Sokolov.[1] More detailed investigations with high-resolution and sensitive apparatus are reported in Refs. 2–5 References 1–5 describe detailed studies of recombination radiation produced upon decay of excitons bound to individual atoms in germanium. These studies have established quite reliably the energy structure of the donors (2*S* states and others) and of the excitons bound to them in germanium. The emission produced in radiative decay of multiparticle electron-impurity complexes (MEIC) in germanium has so far been the subject of much fewer and less detailed studies. This is understandable, for the lines of this emission are much less intense than those of the principal lines of the bound exciton.[4] The radiation produced in moderately and strongly doped germanium crystals[6] has likewise hardly been investigated.[1)] The small contribution of MEIC in germanium to recombination radiation notwithstanding, their study is undoubtedly of interest. This is due, on the one hand, to the peculiarities of the germanium band structure, and on the other to the different energy scale as compared with silicon. This holds in particular for the interaction between the particles in the MEIC, which is comparable[4,5] with the spacings of the principal terms in the MEIC and cannot be considered small as in the case of silicon.[7,8] We present here results of investigations of the low-temperature luminescence of germanium crystals doped with arsenic, phosphorus, and antimony at densities 10^{14}–10^{16} cm^{-3}. In most experiments the samples were uniaxially deformed in the [111] and [001] directions. In some cases the samples investigated were placed in a magnetic field. In the first part of the paper we give the results of our investigations of germanium samples containing small amounts of impurity centers. In the second part we consider the changes produced in the emission spectra when the density of the dopant is increased.

2. EXPERIMENT

The investigated germanium crystals, doped with arsenic, phosphorus, and antimony, were drawn from a germanium melt in a stream of pure hydrogen by the Czochralski method. The samples for luminescence investigations were cut along the [111] and [001] crystallographic directions as parallelepipeds measuring $20\times2\times2$mm. The procedure used to produce the uniform strain and the magnetic field is described in Ref. 8. The samples were etched in a $1H_2O_2 + 1HF + 4H_2O$ mixture. In addition, we measured the resistivity at the centers of the samples, to be able to determine the impurity-center density in the investigated sample region from the known[9] dependence of the resistivity on the donor density. The type of dopant was monitored against the positions of the $\alpha_1(1S)$ and $\alpha_1(2S)$ emission lines of the bound excitons. When the $\alpha_1(1S)$ line was the monitor, an interference procedure[8] of sufficient resolution for this purpose, $\sim 30\,\mu$eV, was used. In the second case we used an ordinary grating spectrometer. The samples were placed in the helium bath of the cryostat. By pumping off the liquid-helium vapor we could vary the helium-bath temperature from 4.2K to below the λ point.

The recombination radiation spectra were analyzed with an SDL-1 double monochromator. When higher resolution was needed we used, as in Ref. 8, an IT-28-30 interferometer. To scan the emission spectra, the interferometer was placed in a chamber filled with a gas whose pressure could be continuously varied. The standard mirrors of the IT-28-30

 0038-5646/85/030501-08$04.00

interferometer were replaced by with mutilayer- dielectric-coated mirrors having a maximum reflectance at 1.7 μm. The interferometer was tuned against the yellow light of a low-pressure sodium lamp. The wavelength of this line is approximately one-third that at the maximum reflectance of our mirrors. This ensured high reflectance at this wavelength and permitted the interferometer to be focused in visible light. In contrast to Refs. 7 and 8, the interferometer was placed at the entrance of the MDR-3 monochromator, whose resolution was relatively low. This placement made for a substantially stronger useful signal and better resolution than in an ordinary grating spectrometer. As a result we had a resolution 2–3 times better than in Refs. 3 and 10.

The samples were excited with an LG-106M-1 argon laser whose emission was mechanically chopped at 72 Hz. The recombination radiation was recorded with a liquid-nitrogen-cooled photoreceiver.[11] The modulated part of the photoresponse was fed through a tuned amplifier and a lock-in detector to the chart of an automatic potentiometer.

3. ANALYSIS OF RECOMBINATION RADIATION SPECTRA OF GERMANIUM CRYSTALS CONTAINING SMALL AMOUNTS OF ARSENIC AND PHOSPHORUS

The recombination-radiation spectra of undeformed germanium containing small amounts of arsenic and phosphorus have been well investigated. We shall therefore concentrate hereafter on the analysis of the emission spectra of uniaxially compressed spectra.

Figure 1 shows the no-photon (*NP*) and phonon (*LA*) components of the recombination radiation spectra of germanium samples doped with arsenic and phosphorus and uniaxially compressed along [001]. The figure shows also the MEIC decay scheme without allowance for the strain and

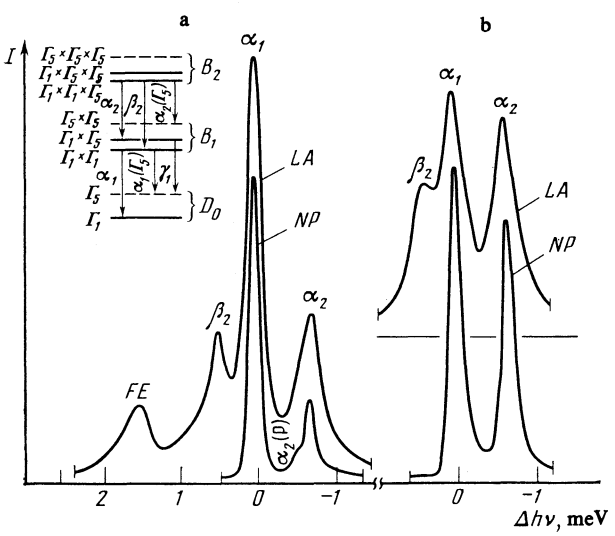

FIG. 1. *NP* and *LA* components of MEIC emission spectrum in germanium at 2 K compressed in the [001] direction (the maxima of the *NP* and *LA* lines are aligned for convenience): a—germanium doped with arsenic at density $4\cdot10^{14}$ cm^{-3} at pressure $2.2\cdot10^3$ kg/cm^2; b—germanium doped with phosphorus at a density $3.5\cdot10^{14}$ cm^{-3} at pressure $1.7\cdot10^3$ kg/cm^2. In the upper left is shown the optical-transition scheme in the MEIC without allowance for deformation and for the particle interaction in the MEIC. The solid and dashed lines show the states stemming from the ground and excited 1*S*-like states of the donor.

for the carrier interaction in the MEIC. The labels on the lines conform to the radiative-transition types of the shell model.[12] the *FE* band is produced by radiative decay of the free excitons. Its width is of the order of kT and is governed by the free-exciton thermal motion. The α_1 lines stem from radiative decay of excitons bound to neutral arsenic and phosphorus atoms.

The intensities of the no-phonon lines α_2 and of the phonon lines α_2 and β_2 increase synchronously with increase of pressure and of the excitation level and with lowering of temperature. This behavior of these lines indicates that they are produced via radiative decay of the exciton-impurity complex B_2 that results from capture of two excitons by a neutral center. The appearance of the complex B_2 when the crystal is compressed in the [001] direction is quite natural, for compression in this direction splits only the valence band (we neglect the splitting of the Γ_5 states), and the degree of band degeneracy allows the existence of B_2 complexes containing three electrons and two holes. Note that this situation is similar to that in phosphorus-doped silicon compressed in the [111] direction.[13] We recall that α_2 lines are observed in both the phonon and the no-phonon component of the spectrum and are due to radiative decay of the complex B_2, a decay that results in a bound exciton in the excited state. The β_2 line is located at the short-wave edge of the bound-exciton line, i.e., just as in the case of undeformed silicon. This indicates that the binding energy of the second exciton in the B_2 complex is less than of that in B_1. It follows from Fig. 1 that the energy of binding the excitons in complexes B_1 and B_2 to the donors (D_0) arsenic and phosphorus are 1.4 and 0.9 meV and 1.36 and 0.85 meV, respectively. The energy needed to excite a bound exciton is determined from the locations of the lines α_2 and β_2 in the spectrum and equals 1.23 and 1.05 meV for excitons bound to arsenic and phosphorus, respectively.

We examine now the spectrum region shown in Fig. 2 and corresponding to a bound-exciton decay that causes one donor to remain in one of the excited states Γ_5, 2*S*, 3*S*, etc. If the energy is measured from that of the 1*S* state, the energies corresponding to these states are 4.3, 10, and 11.7 meV. The arrow in Fig. 2 marks the energy at which the discrete spectrum of the antimony goes over into the continuous spectrum of the conduction band. The fact that the spectral density of the radiation exceeds the background at this point suggests apparently that the radiative decay of a bound exciton can terminate in ejection of the remaining electron from the donor into the conduction band.

In Fig. 3 are shown the dependences of the positions of the bound-exciton lines on the pressure applied in the [111] direction. (A typical spectrum at intermediate pressures is shown in Fig. 7 below.) It can be seen from Fig. 3 that increasing the pressure excites a number of lines and shifts them nonlinearly.

Pressure decreases sharply the bound-exciton line intensity at 4.2 K. This is particularly true of phosphorus-doped germanium crystals. The lower intensity of these lines can be understood by recognizing (see below) that deformation of germanium in the [111] direction should lower the binding energy of the bound exciton by $\sim 3/4\Delta_0'$(Δ_0' is the

energy between the Γ_1 and Γ_5 levels in an exciton bound to a donor). This lowers the exciton-arsenic and exciton-phosphorus binding energies to 0.42 and ~ 0.29 meV, respectively. Thus, at 4.2 K these energies are comparable with kT and the thermal motion should destroy the bound excitons. Lowering the temperature to 2 K increases abruptly the bound-exciton emission-line intensities, and this is also explained by the foregoing arguments.

As already noted, the final decay state B_1 is that of a neutral donor in the ground or in one of the excited states. In the absence of strain, the ground state of an electron bound to arsenic is split into two states, Γ_1 (singlet) and Γ_5 (triplet). The distance between the levels Γ_1 and Γ_5 is $\Delta_0 = 4.33$ meV. Compression in the [111] direction splits the state Γ_5 into a doublet Γ_3 that shifts[14] like $-\frac{1}{4}\Delta_0 x$ (where $x = \frac{8}{9}\Xi_u \varepsilon_{111}/\Delta_0$; Ξ_u, and Ξ_d are the constants of the deformation potential, and ε'_{111} is the relative deformation), while the singlet states shift like $\frac{1}{2}\Delta_0[-1+x/2+(1+x+x^2)^{1/2}]$.

The state Γ_1 corresponding to the singlet state of the undeformed crystal shifts like $\frac{1}{2}\Delta_0[-1+x/2-(1+x+x^2)^{1/2}]$. The wave functions in then deformed crystal are the linear combinations of the wave functions of the undeformed crystal.

The foregoing expressions allow us to calculate the excited-donor following deformation in the [111] direction. The changes produced in the donor levels by deforming the germanium in the [111] direction, calculated from these equations, are shown in the upper left of Fig. 3. One can expect[8] to observe in the B_1 emission spectrum lines corresponding to donor production not only in the ground but also in excited states. The lines should be shifted towards lower energies relative to the α_1 line, by an amount equal to the donor excitation level. For the $\alpha_1(\Gamma_5)$ line corresponding to donor production in a Γ_3 state, this shift is equal to

$$\Delta(\Gamma_5) = \Delta_0(1+x+x^2)^{1/2}, \qquad (1)$$

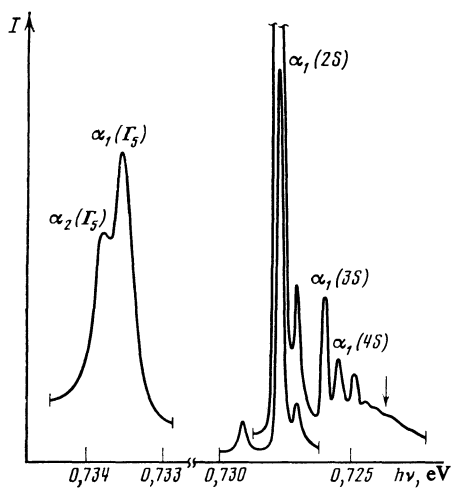

FIG. 2. *NP* components appearing of the emission spectrum of germanium doped with arsenic at a density $1\cdot10^{14}$ cm^{-3} as a result of radiative decay of the complexes B_1 and B_2, with production of a donor D_0 in excited states. Temperature $T = 2$ K, pressure 2190 kgf/cm^2 applied in the [001] direction.

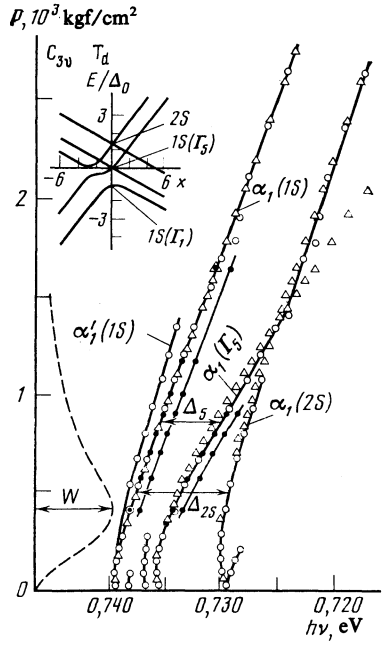

FIG. 3. Location of *NP* bands in the recombination-radiation spectrum of germanium doped with $4\cdot10^{15}$ cm^{-3} of arsenic as a function of the pressure applied in the [111] direction. The experimental points were obtained at temperatures 4.2 K (○) and 2 K (△); ▽—calculated from the equations given in the text. W is the square of the overlap integral as a function of the applied pressure. In the upper left is shown the donor energy-level splitting scheme following compression of the germanium crystals in the [111] direction with allowance (in compression) for the interaction between the $1S$ and $2S$ levels.

and for the $\alpha_1(2S)$ line, assuming weak splitting (~ 0.5 meV) of the $2S$ state in the deformed crystal, it is equal to

$$\Delta(2S) = \tfrac{1}{2}\Delta_0[1+x+(1+x+x^2)^{1/2}]+\Delta', \qquad (2)$$

where Δ' is the difference between the energy needed to excite the $2S$ state and Δ_0. The values calculated in this manner are represented by the triangles of Fig. 3. It can be seen from the figure that the $\alpha_1(\Gamma_5)$ line is indeed observed in the spectrum, and its position agrees satisfactorily with the calculation at low pressures. The $\alpha_1(\Gamma_5)$ is almost nonexistent in the spectrum of undeformed germanium. When pressure is applied in the [111] direction the intensity of this line increases strongly. In addition, at pressures on the order of 10^3 kgf/cm^2 the behavior of this line changes to that of the $\alpha_1(2S)$ line.

For a better understanding of the phenomena we observed, we shall use hereafter the following simplified model of a bound exciton. We shall assume that the wave function of a bound exciton, in either a deformed or an undeformed crystal, can be approximately be made up of single-particle wave functions that are solutions of the single-particle Schrödinger equation corresponding to electron motion in an effective potential field. We assume here[7,8] that the orbitals that make up the bound-exciton wave functions have the symmetry of the $1S$-like wave functions of an electron on a donor. In addition, we assume that one orbital is close to one of the wave functions of the electron on the donor, and the other spans a larger space. We write by way of example the bound-exciton ground-state wave function:

$$\Psi_{\text{b.e.}}=\psi^h(r_h)\,\psi^e(r_1,\,r_2)=\psi_{\Gamma_8}{}^h(r_h)\,\{\psi_{\Gamma_1}(r_1)\,\psi_{\Gamma_1}{}^D(r_2)\}\,[\alpha(1)\,\beta(2)\,], \tag{3}$$

where $\psi^D_{\Gamma_1}(r)$,$\psi_{\Gamma_1}(r)$ and $\psi^h_{\Gamma_8}(r_h)$ are the single-particle wave functions of the electrons and of the hole, and transform in accordance with the irreducible representations of Γ_1 and Γ_5. The curly and square brackets are the respectively symmetrized and antisymmetrized products of the functions, and α and β are spin wave functions corrsponding to different orientations of the electron spin. The remaining wave functions that describe the excited states of the carriers in the MEIC are similarly constructed. In the optical-transition scheme (Fig. 1) they are arbitrarily marked by the representations according to which the spatial part of the electron wave function is transformed. In the approximation we are using, the probability amplitude of a bound-electron radiative decay should be proportional to[12]

$$d_{j1}\langle\hat{K}\psi^h|\hat{P}|\psi_1\rangle+d_{j2}\langle\hat{K}\psi^h|\hat{P}|\psi_2\rangle. \tag{4}$$

Here $d_{ji}=\langle\psi^D_j|\psi_i\rangle$ are the overlap integrals of the single-particle wave functions of the bound exciton and the wave functions of the electron in the neutral donor, $\hat{P}$ is the electron-photon interaction operator, and $\hat{K}$ is the time-reversal operator.

We return now to Fig. 3. According to the model considered, the bound-exciton line α_1 should undergo, with increase of pressure, an additional short-wave shift $\sim\frac{3}{4}\Delta_0'$, as is indeed verified by Fig. 3. We consider now the behavior of the $\alpha_1(\Gamma_5)$ line. As already noted, this line is excited as the pressure is increased. In this approximation, the bound-exciton line intensity is proportional to the squared modulus of the probability amplitude (4). Since the different donor wave functions are orthogonal, the overlap integral $\langle\psi^D_{\Gamma_5}|\psi^D_{\Gamma_1}\rangle$ vanishes. The transition probability will therefore be proportional to the squared modulus of the second overlap integral $\langle\psi^D_{\Gamma_5}|\psi_{\Gamma_1}\rangle$, which can be written, in view of its pressure dependence, in the form

$$(\alpha\beta+3)\,[\,(3+\beta^2)\,(3+\alpha^2)\,]^{-1/2}, \tag{5}$$

where

$$\beta=3/[1+2x-2(1+x+x^2)^{1/2}],\ \alpha=-1-2x'+2(1+x'+x'^2)^{1/2},\quad x'=x(\Delta_0/\Delta_0').$$

We have designated the squared overlap integral (5) by W and show it in Fig. 3. It can be seen that the $\alpha_1(\Gamma_5)$ line should first flare up and then damp away. Experiment shows a different picture. The line in question is indeed strongly flared up, but with further increase of pressure its intensity remains approximately constant. To resolve this contradiction, we turn to the level-splitting scheme shown in Fig. 3. for donor levels of germanium uniaxially deformed in the [111] direction. In this deformation, the donor state Γ_5 is split in the c_{3v} group into states Γ_3 and Γ_1, while a state Γ_1 spilts off from the state $2S$ and moves downward. At

$$x_0=-\frac{4p(1+p)}{1+4p}\approx-2,\qquad p=\frac{\Delta'}{\Delta_0}\approx 1.37$$

according to the equation above, the two Γ_1 states from different levels should cross on the scheme of Fig. 3. This, however, is not the case experimentally. The $\alpha_1(2S)$ line drops off as it approaches the $\alpha_1(\Gamma_5)$ line, while the latter behaves past the intersection point as the $\alpha_1(2S)$ line should. This behavior of the lines can be understood by recalling the quantum-mechanical theorem[15] according to which two terms of like symmetry and belonging to a Hamiltonian that depends on one parameter cannot intersect. The wave functions of these terms are intermixed at the "intersection" point, and it is this which explains the effects observed. In our case the interaction of the $1S$ and $2S$ states is due to the interaction of the electron with central-cell field. With allowance for the deformation, this interaction can be written in the form

$$H=-\Delta'\sigma_2\times I_4-\Delta_0\sigma_2\times I_1'+\Delta_1\sigma_x\times I_1'+\Delta_2\sigma_x\times I_4+\Delta_0 I_2\times H_\varepsilon, \tag{6}$$

where Δ_1 and Δ_2 are constants that describe the interaction of the $1S$ and $2S$ states; I_n is a unit matrix of dimensionality n, and I_1' is a four-dimensional matrix with all elements equal to 1/4;

$$\sigma_2=\begin{pmatrix}0&0\\0&1\end{pmatrix},\qquad \sigma_x=\begin{pmatrix}0&1\\1&0\end{pmatrix};$$

H_ε is a four-dimensional matrix whose diagonal elements are the energies ΔE^α of the displacements of the conduction-band minima by a pressure P applied along the $[11n]$ direction. Apart from a term $(\Xi_d+\frac{1}{3}\Xi_u)\mathrm{Tr}\varepsilon$ that is constant for all the minima, the displacement energies are

$$\begin{aligned}\Delta E(111)&=\tfrac{2}{3}\Xi_u(\varepsilon_{xy}+2\varepsilon_{xz}),\\ \Delta E(\bar{1}11)=\Delta E(1\bar{1}1)&=-\tfrac{2}{3}\Xi_u\varepsilon_{xy},\\ \Delta E(\bar{1}\bar{1}1)&=\tfrac{2}{3}\Xi_u(\varepsilon_{xy}-2\varepsilon_{xz}),\end{aligned} \tag{7}$$

where

$$\varepsilon_{xy}=\frac{S_{44}P}{2(n^2+2)},\qquad \varepsilon_{xz}=\varepsilon_{yz}=\frac{nS_{44}P}{2(n^2+2)}, \tag{8}$$

$\mathrm{Tr}\,\varepsilon=(S_{11}+2S_{12})P$, and ε_{ij} is the strain tensor.

Solution of the equation $|H-EI|=0$ enables us to determine the behavior of the $1S$ and $2S$ donor levels as a function of the pressure applied to the crystal. Comparison of our calculations with the experimental results provided estimates of the constants that describe the interaction of the electron with the field of the central cell. If it is assumed[14-16] that $\Delta_1\gg\Delta_2$, we have $\Delta_1\sim 1.5$ meV.

Our model provides also a natural explanation of the appearance of the $\alpha_2(\Gamma_5)$ line shown in Fig. 2). The intensity of this line is approximately 300 times smaller than that of α_1. This line can be attributed to decay of the complex B_2, which leads to creation of a bound exciton. The internal orbital of this exciton is close to the wave function of the a donor with the symmetry of Γ_5. To prove that the line stems from the decay of the complex B_2, we used a constant background illumination method.[17] This illumination was provided by a second argon laser whose output was focused in the region excited by the main Q-switched argon laser. Addition of constant background decreased the intensity of the line α_1 and increased that of line α_2. The altered intensities of the lines $\alpha_1(\Gamma_5)$ and $\alpha_2(\Gamma_5)$ caused the line $\alpha_2(\Gamma_5)$ to predominate. By varying the intensity of the background illumination we could change the amplitude ratio of the lines $\alpha_1(\Gamma_5)$ and $\alpha_2(\Gamma_5)$.

We consider now the interaction of carriers in MEIC in germanium. It follows from Ref. 3 that interaction of carri-

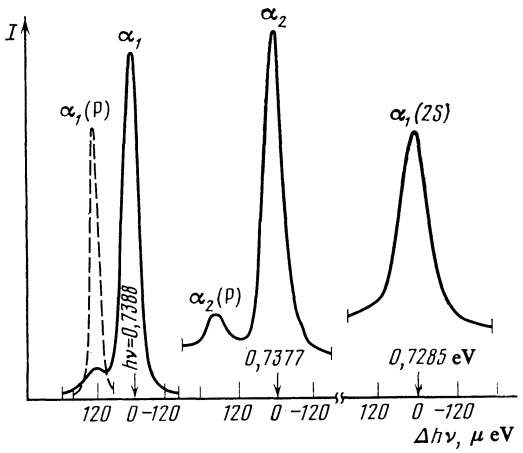

FIG. 4. Spectral distribution of *NP* components of the recombination radiation of complexes B_1 and B_2 in germanium samples doped with arsenic or phosphorus at $T = 2$ K and compressed in the [001] direction: solid line—germanium doped with $4\cdot10^{14}$ cm^{-3} arsenic at $2.34\cdot10^3$ kgf/cm^2; dashed line—germanium doped with $3.5\cdot10^{14}$ cm^{-3} phosphorus at $3.6\cdot10^2$ kgf/cm^2.

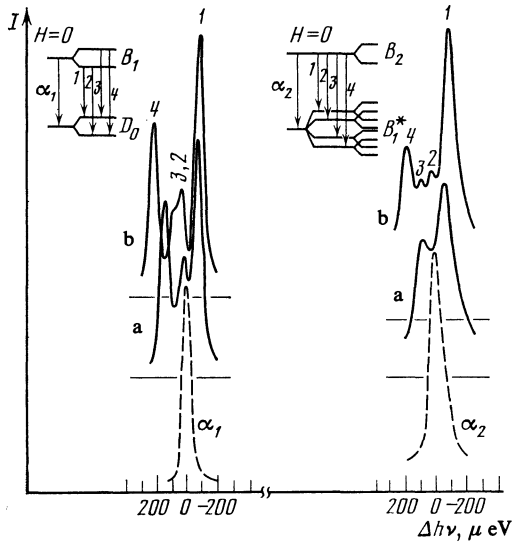

FIG. 5. Zeeman splitting of the recombination-radiation $NP - \alpha_1$ and $NP - \alpha_2$ lines of the complexes B_1 and B_2 for phosphorus atoms in germanium deformed by $2.35\cdot10^3$ kgf/cm^2 pressure along [001] at $T = 2$ K and at a phosphorus density $3.5\cdot10^{14}$ cm^{-3}. Line α_1: dashed—$H = 0$ kOe; a—$H = 12.5$ kOe; b—$H = 17.8$ kOe; line α_2: dashed—$H = 0$ kOe; a—$H = 8.2$ kOe; b—$H = 15.3$ kOe. The spectra were obtained in the Voigt configuration. The particle interactions in the MEIC are not taken into account in the optical level schemes of the insets.

ers in MEIC in undeformed germanium causes an energy-level splitting comparable with the energy spacing of the levels. We have attempted to investigate the fine structure of the MEIC emission lines from donors in germanium deformed along [001]. When germanium is compressed in this direction the conduction band remains unchanged, and the valence band splits into two doubly degenerate bands. There was hope therefore that such a strain would simplify the spectrum obtained in Ref. 3 and lead to more specific conclusions on the carrier interaction in MEIC in germanium. To obtain spectra in which the fine structure of the energy levels in the MEIC could be resolved, we used the interference technique described above.

Figures 4 and 5 show the emission spectra of the complexes B_1 and B_2 in germanium doped with arsenic and with phosphorus. It can be seen from the figure that the arsenic-doped sample contains also traces of phosphorus. The widths of the α_1 lines shown in Figs. 4 and 5 are determined mainly by the inhomogeneity of the sample deformation. For comparison, Fig. 4 shows the $\alpha_1(P)$ line of excitons bound to phosphorus atoms in weakly deformed germanium. This line is much narrower, and its half-width is less than $30\,\mu$ eV and is determined by the interferometer instrumental function. The half-widths of lines α, and α_2 are 55 and $110\,\mu$ eV respectively in Fig. 4 and 67 and $110\,\mu$ eV in Fig. 5.

It was observed in Ref. 3 that the α_1 line consists of several well-resolved components. It can be seen from Figs. 4 and 5 that in germanium compressed along [001] the α_2 lines is respresented in the recombination-radiation spectrum by only one component.[2)] It can also be seen that the α_2 line is noticeably broadened. This suggests that it consists of several components that we did not resolve. It can be assumed here that all the line components are contained in the lines shown in Figs. 4 and 5.

This assumption is confirmed by analysis of the Zeeman-splitting spectra we obtained for these lines. It was found that in germanium deformed along [001] the complex B_2 contains two electrons and two holes in singlet Γ_1 states and one electron in the Γ_5 state. The initial state of the complex B_2 is therefore split in a magnetic field into two. A bound exciton B_1 in the excited state is left following radiative decay of the complex B_2. The exciton B_1 contains one electron in the Γ_1 state, one electron in the Γ_5 state, and one hole in the Γ_6 state. The final state is split in the magnetic field as shown in Fig. 5. It can be seen from the figure that only four components should be observed in the emission spectrum. The Zeeman spectrum shown in Fig. 5 contains in fact four components, thereby confirming our assumption. We note that the arguments advanced are valid when the particle interaction in the MEIC is weak. Otherwise we must use a transition scheme similar to that given in Ref. B. More detailed information on MEIC emission spectra in germanium can be found in Ref. 10.

The fact that the α_2 line of germanium deformed along [001] has only one component was unexpected, since one could expect according to Ref. 18 the main features of the splitting observed in Ref. 3 to remain unchanged. Indeed, when germanium is deformed in this direction the conduction band remains unchanged, so that there should likewise be no change inthe *ee* interaction that causes, according to Ref. 18, the α_2-line splitting observed in Ref. 3. It follows hence that the α_2-line splitting observed in undeformed germanium is determined mainly by an *eh* interaction similar to that in the exciton and leading to crystalline splitting. In germanium deformed along [001] this interaction is "turned off" and the α_2 broadening observed by us can be attributed to "weak" *ee* (Ref. 18) and *eh* (Ref. 8) interactions.

We note in conclusion that if it is assumed that the broadening we observed of the $\alpha_2(2S)$ line (see Fig. 4) is not caused by strain or density (see Sec. 4 below), it can be attri-

buted to the short lifetime of the electron in the excited $2S$ state.[8] We find then from the uncertainty principle and from the broadening, which is easily gotten from Fig. 4, that the electron lifetime in the $2S$ state is of the order of $3\cdot10^{-11}$ s.

4. ANALYSIS OF RECOMBINATION-RADIATION SPECTRA OF GERMANIUM MODERATELY DOPED WITH ARSENIC, PHOSPHORUS, AND ANTIMONY

We note first that an increase of the dopand density is accompanied by an increase of the "background" in the recombination radiation, i.e., by a nonresonant increase of the recombination radiation intensity. The "background" complicates considerably the investigation of the low-intensity emission lines of the spectrum. At the same time, an increased impurity density broadens the recombination radiation lines. Figure 6 shows a plot of a bound-exciton NP-α_1 line half-width vs the arsenic and phosphorus densities in germanium. It can be seen from the figure that a noticeable line broadening sets in at a density on the order of 10^{15} cm^{-3}. The observed inhomogeneous line broadening can be naturally attributed to interactions between the bound excitons and the surrounding impurity centers. In addition, raising the density of the impurity centers leads also to the appearance of a number of new lines in the recombination-radiation spectrum.[2,6,19]

It was shown in Ref. 19 that new luminescence lines, close to those of the bound exciton, were observed at $T = 2$ K in germanium crystals moderately doped with arsenic, phosphorus, and antimony. These lines are inhomogeneously broadened towards the longer wavelengths and their maxima are shifted by approximately 1 meV towards lower energies. The new radiation is easier to observe in uniaxially deformed germanium crystals doped with arsenic, at relatively low excitation levels, when the electron-hole drops (EHD) contribute little to the radiation.

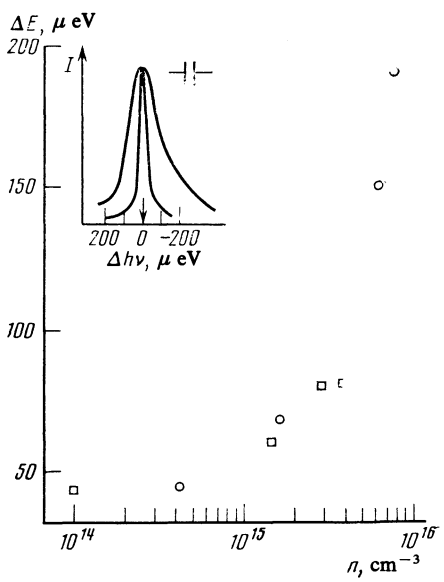

FIG. 6. Half-width of $NP-\alpha_1$ line of a bound exciton in germanium vs the impurity atom density at $T = 4.2$ K: □—arsenic-doped germanium; ○—phosphorus-doped germanium. The inset shows two spectra of the α_1 line of excitons bound in germanium doped with phosphorus at densities $3.5\cdot10^{14}$ cm^{-3} (narrow line) and $8\cdot10^{15}$ cm^{-3} (broad line).

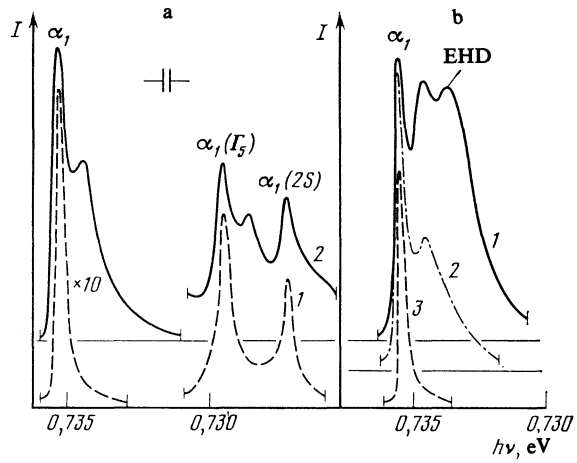

FIG. 7. Spectral distribution of recombination-radiation NP components of germanium doped with $4\cdot10^{15}$ cm^{-3} of arsenic and compressed along [111] at 740 kgf/cm^2. The new-radiation band has no index. a) Low excitation level $1-T=4.2$ K, $2-T=2$K; b) high excitation level: $1-T=2$ K, $2-T=2.8$ K, $3-T=4.2$ K.

In contrast to the lines α_1 and β_1, which are observed only when the crystals are compressed along [001], the new lines are present in the spectra regardless of the uniaxial deformation direction. Figure 7 shows luminescence spectra of germanium doped with arsenic at a density $4\cdot10^{15}$ cm^{-3}. It can be seen from Fig. 7a that the new radiation is barely observed at 4.2 K but is clearly seen when the temperature is lowered to 2 K in the no-phonon region, including near the $\alpha_1(\Gamma_5)$ line corresponding to decay of a bound exciton and creation of a donor in the excited state. With increasing excitation level, the intensity of the new line varies approximately in the same manner as that of the bound-exciton line. At high excitation levels (Fig. 7b) and at low temperatures, a line appears in the spectrum and can be attributed to EHD radiation.[20] When the temperature is raised, the first to vanish is the EHD band, followed by the new-radiation band.

Figure 3 shows a plot of the spectral arrangement of the new lines vs the applied pressure. The new bands can be seen to shift with increasing pressure, in analogy with the shifts of the lines α_1 and $\alpha_1(\Gamma_5)$. It follows therefore that a neutral donor participates in the recombination act responsible for the production of the new band and can become excited as a result. We note also that, unlike the lines α_2 and β_2 (see Fig. 4), the new band has a "tail" that extends into the low-energy region. The LA-phonon emission spectrum of this band, produced when the crystals are compressed along [001] and [111], is similar to the NP-component spectrum. Similar emission bands are observed also in germanium crystals doped with phosphorus and antimony. In contrast to crystals doped with arsenic and phosphorus, the intensity of the NP component in antimony-doped crystals is significantly lower than that of the LA component.

We examine now the influence of the dopant density on the new lines. Figure 8 shows the evolution of the recombination-radiation spectra of germanium doped with arsenic (Fig. 8a) and phosphorus (Fig. 8b) as the densities of these impurities are varied in the germanium crystal. All the spectra of Fig. 8 were obtained under approximately the same

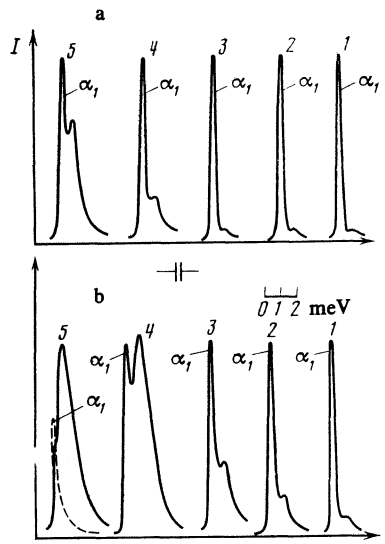

FIG. 8. Evolution or recombination-radiation *NP* components for germanium doped with arsenic and phosphorus and compressed along [111] at 980 kg/cm^2, at $T = 2$ and at approximately equal photo-excitation levels. a) Germanium doped with arsenic at densities: 1—$n = 10^{14}$ cm^{-3}, 2—$n = 3\cdot10^{14}$ cm^{-3}, 3—$n = 7\cdot10^{14}$ cm^{-3}; 4—$n = 1.5\cdot10^{15}$ cm^{-3}, 5—$n = 4\cdot10^{15}$ cm^{-3}; b) germanium doped with phosphorus at densities: 1—$n = 4\cdot10^{14}$ cm^{-3}, 2—$n = 1.5\cdot10^{15}$ cm^{-3}, 3—$n = 2\cdot10^{15}$ cm^{-3}, 4—$n = 8\cdot10^{15}$ cm^{-3}, 5—$n = 1.5\cdot10^{16}$ cm^{-3}. The spectrum obtained at $T = 4.2$ K is shown dashed.

conditions. It can be seen that the intensity of the new lines increases with increasing density. The fact that the new lines have a density-dependent intensity precludes their being attributed to radiative decay of excitons bound to individual centers, and eliminates the explanation proposed in Ref. 19 as well.

To verify the foregoing conclusion, we investigated germanium samples doped with both antimony and arsenic. The antimony density was chosen so that the perdominant radiation was due to excitons bound to arsenic atoms in the no-phonon part and to excitons bound to antimony in the phonon part. The arsenic density was chosen low enough to eliminate it as a cause of radiation from the germanium.

Figure 9 shows the *NP* and *LA* components of the emission spectra of a germanium sample doped with antimony

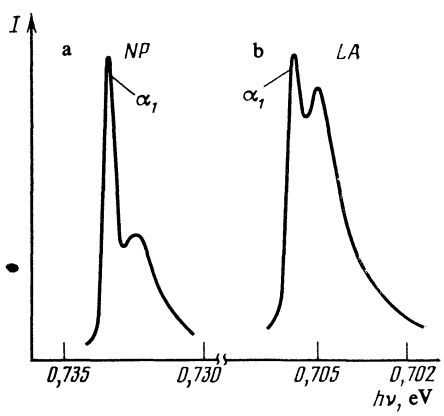

FIG. 9. Spectral distribution of recombination-radiation *NP* and *LA* components of recombination radiation of germanium doped with both antimony and arsenic at densities $3.5\cdot10^{15}$ cm^{-3} and $\sim10^{14}$ cm^{-3} and compressed along [111] at 970 kgf/cm^2 at $T = 2$ K.

and arsenic at densities satisfying the foregoing conditions. It can be seen from the figure that the new-radiation bands are present not only in the phonon part of the spectrum but also in the no-phonon part. It follows hence that the onset of new radiation calls for the presence of at least a pair of impurity atoms, not necessarily identical. Indeed, as can be seen from Fig. 8 the new lines become dominant in the emission spectrum at densities on the order of $5\cdot10^{15}$ cm^{-3}. At such densities the average distance between impurities is of the order of $5\cdot10^{-6}$ cm, or comparable with the Bohr radius of the bound exciton. In this situation one can expect the crystal to contain many impurity pairs in which the distance between the impurity atoms is of the order of the Bohr radius of the bound exciton. This is also attested to by the bound-exciton line broadening observed at such densities (see Fig. 6).

Our experimental results can be satisfactorily explained by assuming that the new radiation is due to radiative decay of an exciton bound to a pair of impurity centers. One can expect in this case (in agreement with the spectral arrangement and the profiles of the new emission bands) that such an exciton has a binding energy higher than that of an exciton bound to an isolated donor, and that this energy will increase with decreasing distance between the atoms of the pair. Since in practice there is no difference whatever between the binding of an exciton to a pair of atoms and binding to an isolated impurity, it becomes clear why the intensities of the new band and of the bound-exciton line have the same dependence on the excitation level. The onset of this radiation alongside the $\alpha_1(\Gamma_5)$ line also finds a natural explanation. Indeed, if this radiation is due to radiative decay of an exciton bound to a pair, two neutral donors should be produced, and one can go over into the excited state Γ_5.

It is somewhat more difficult to explain the temperature dependence of this radiation. We introduce the following notation. Let N_1, N_2, n_1, and n_2 be respectively the densities of the isolated centers, of the pairs, of the bound excitons, and of the excitons bound to atom pairs; let also E_1 and E_2 be the respective binding energies of the excitons with isolated atoms and with pairs. The radio of the intensity I_2 of the emission of excitons bound to pairs to the intensity I_1 of exciton bound to individual centers is then, in the stationary case,

$$\frac{I_2}{I_1} = \frac{(1-n_2/N_2)}{(1-n_1/N_1)}\frac{N_2}{N_1}\exp\left(\frac{E_2-E_1}{kT}\right). \tag{8}$$

Under the conditions of our experiments, n_2/N_2, $n_1/N_1 \ll 1$, $N_2/N_1 \approx 10^{-2}$ and $E_2 - E_1 = 0.8$ meV. This yields $I_2/I_1 \approx 10^{-2}$, at 4.2 K and $I_2/I_1 \sim 1$ at 2 K, in satisfactory agreement with experiment. The new radiation can thus be attributed to radiative decay of excitons bound to impurity pairs. We note that radiative decay of complexes produced at an impurity pair by capturing more than one exciton cannot be excluded as a cause of this radiation.

We note in conclusion that we observed similar radiation in silicon doped with phosphorus at a density 10^{17} cm^{-3}. The maximum of this radiation is shifted approximately 1 meV downward in energy relative to the $NP - \alpha_1$

line of a bound exciton. When the temperature was lowered from 4.2 to 2K its intensity increased and exceeded the bound-exciton line intensity.

The authors thank Ya. E. Pokrovskiĭ and G. E. Pikus for a detailed discussion of the work and for a much valuable advice, A. M. Kogan for a discussion of electron interaction with the field of the central cell, and A. B. Lopatin, V. A. Karasyuk, and V. G. Leĭtes for programming the data acquisition and reduction. Particular thanks is due to T. P. Elagina for growing practically all the germanium crystals used in the present study.

[1)]Weakly, moderately, and strongly doped crystals are taken here to mean those in which the distances between the impurities are much larger, of the order of, and less than the Bohr radius of the exciton.

[2)]A recent paper[10] is devoted mainly to nonstationary bound "biexcitons" in germanium. It includes nevertheless also spectra of the $NP - \alpha$ line and its Zeeman components for the complex B_2 in germanium doped with arsenic and compressed along [001]. These spectra agree with ours and contain no additional structure. We note that the lines $LA - \alpha_2$ and $LA - \beta_2$ of the usual complexes B_2 are not given in Ref. 10.

[1]E. F. Gross, B. V. Novikov, and N. S. Sokolov, Fiz. Tverd, Tela (Leningrad) **14**, 443 (1972) [Sov. Phys. Solid State **14**, 368 (1972)].
[2]R. W. Martin, Solid St. Commun. **14**, 369 (1974).
[3]A. E. Mayer and E. C. Lightowlers, J. Phys. **C12**, L945 (1979).
[4]A. E. Mayer and E. C. Lightowlers, *ibid.* **C13**, L747 (1980).
[5]A. E. Mayer and E. C. Lightowlers, 15th Conf. Semicond. Physics, Kyoto, 1980; J. Phys. Soc. Japan **49**, Suppl. A, 441 (1980).
[6]R. W. Martin and R. Sauer, Phys. Stat. Sol. (b) **62**, 443 (1974).
[7]A. S. Kaminskii, V. A. Karasyuk, and Ya. E. Pikrovskiĭ, Pis'ma Zh. Eksp. Teor. Fiz. **33**, 141 (1981) [JETP Lett. **33**, 132 (1981)].
[8]A. S. Kaminskii, V. A. Karasyuk, and Ya. E. Pokrovskiĭ, Zh. Eksp. Theor. Fiz. **83**, 2237 (1982) [Sov. Phys. JETP **56**, 1295 (1982)].
[9]Tablitsy fizichskikh velichin (Tables of Physical Quantities), Atomizdat 1976, p. 352.
[10]I. E. Itskevich and V. D. Kulakovskiĭ, Fiz. Tverd. Tela (Leningrad) **26**, 496 (1984) [Sov. Phys. Solid State **26**, 296 (1984)].
[11]A. S. Kaminskiĭ, Ya. E. Pokrovskiĭ, and S. V. Poteshin, Prib. Tekh. Éksp. No. 3, 229 (1977).
[12]G. Kirczenov, Can. J. Phys. **55**, 1787 (1977).
[13]A. S. Kaminskii and Ya. E. Pokrovskiĭ, Zh. Eksp. Teor. Fiz. **75**, 1037 (1978) [Sov. Phys. JETP **48**, 523 (1978)].
[14]G. L. Bir and G. E. Pikus, Symmetry and Strain-Induced Effects in Semiconductors, Wiley, 1975.
[15]L. D. Landau and E. M. Lifshitz, Kvantovaya mekhanika (Quantum Mechanics). Fizmatgiz, 1963, p. 322 [Pergamon, 1965].
[16]W. Kohn and G. M. Luttinger, Phys. Rev. **98**, 915 (1955).
[17]A. S. Kaminskii, V. A. Karasyuk, and Ya. E. Pokrovskiĭ, Zh. Eksp. Teor. Fiz. **74**, 2234 (1978) [Sov. Phys. JETP **47**, 1162 (1978)].
[18] G. E. Pikus and N. S. Averkiev, Pis'ma Zh. Eksp. Teor. Fiz. **32**, 352 (1980) [JETP Lett. **32**, 328 (1980)].
[19]A. S. Kaminskiĭ, Ya. E. Pokrovskiĭ, and M. V. Gorbunov, *ibid.* **36**, 10 (1982) [**36**, 11 (1982)].
[20]Ya. Pokrovskii, Phys. St. Sol. **11a** 385 (1972).

Translated by J. G. Adashko